

A set of basis functions to improve numerical calculation of Mie scattering in the Chandrasekhar-Sekera representation

Alexandre Souto Martinez*

*Faculdade de Filosofia, Ciências e Letras de Ribeirão Preto,
Universidade de São Paulo
Av. Bandeirantes, 3900*

*14040-901, Ribeirão Preto, SP, Brazil. and
National Institute of Science and Technology in Complex Systems (LNCT-SC)*

Tiago José Arruda†

*Faculdade de Filosofia, Ciências e Letras de Ribeirão Preto,
Universidade de São Paulo
Av. Bandeirantes, 3900*

14040-901, Ribeirão Preto, SP, Brazil.

(Dated: May 26, 2022)

Numerical calculations of light propagation in random media demand the multiply scattered Stokes intensities to be written in a common fixed reference. A particularly useful way to perform automatically these basis transformations is to write the scattered intensities in the Chandrasekhar-Sekera representation. This representation produces side effects so that numerical tests are necessary to deal with the limiting situations of the small-particle (Rayleigh) and forward/backward scattering. Here a new set of basis functions is presented to describe the scattering of light by spherical particles (Mie scattering) in the Chandrasekhar-Sekera representation. These basis functions can be implemented in a new algorithm to calculate the Mie scattering amplitudes, which leads straightforwardly to all the scattering quantities. In contrast to the traditional implementation, this set of basis functions implies to natural numerical convergence to the above mentioned limiting cases, which are thoroughly discussed.

PACS numbers: 03.65.Nk, 42.25.Dd, 03.50.De, 02.70.-c

Keywords: Mie scattering, Chandrasekhar-Sekera representation, multiple scattering, random media, radiative transfer equation, Monte Carlo simulation, computation technics

I. INTRODUCTION

The scattering of an electromagnetic plane wave by a spherical (homogeneous, isotropic and optically linear material) particle of arbitrary size is known as Mie scattering [1–4]. The numerical calculation of this scattering is relevant to several fields such as remote sensing (meteorological optics, radar detection of raindrops, lidar detection of clouds etc.) [5], optical particle characterization (inverse problems)[6–9], photonic band gaps materials (PBGs) [10, 11] etc. More recently, magnetic Mie scattering has attracted the attention of researchers [12–21].

In optical dense media, the light scattered by a particle is successively rescattered and the electromagnetic wave phase coherence may not be totally destroyed by the particle configuration averages producing interesting effects due to phase correlation [22]. The role of numerical multiple scattering description is twofold: it can be viewed as a tool in the comprehension of more fundamental aspects (memory of incident polarization state [23–27], weak localization [28–30]) or as a tool for random media charac-

terization (light scattering by biological tissues [31–41], for instance). These procedures demand considerable numerical efforts and it is desirable to have very efficient and robust (covering a wide range of values in the parameter space) codes to perform such tasks.

To deal with numerical multiple scattering simulation, basis transformations must be performed to represent the local scattered Stokes intensities into a common fixed basis, the laboratory basis. For instance, this procedure is successively repeated in multiple scattering of light in a Monte Carlo scheme. Other than being cumbersome, these basis transformations may increase the propagation of round-off errors in the numerical simulations and may ask for complementary tests in limiting situations.

These basis transformations may be implicitly considered writing all the wavevectors in the same laboratory basis. This is the Chandrasekhar-Sekera representation [42, 43], which has been employed either in a radiative transfer equation calculation [44] as well as in a Monte Carlo scheme [45]. The drawback of this representation (not stressed in the literature) is the introduction of new difficulties to numerical calculation, notably the non-commutation of the two limiting cases: *(i)* small particle size compared to the wavelength (important to polydispersion calculations), and *(ii)* forward/backward scattering events (important to variance reduction in a Monte Carlo schemes and radar/lidar detection).

*Electronic address: asmartinez@ffclrp.usp.br

†Electronic address: tiagoarruda@pg.ffclrp.usp.br

In this paper the problem of limits non-commutability is pointed out and a new set of basis functions for Mie scattering calculation is proposed to the implementation of an algorithm. This algorithm naturally includes the small particle size and backward/forward scattering. The presentation is divided as follows. In Section II, a brief review of Mie scattering in the scattering plane representation is presented to set up the notation. Also, an original expansion of the scattering amplitudes up to fourth-order on the cosine of the scattering angle is calculated. In Section III, the Chandrasekhar-Sekera representation is reviewed. It is pointed out in Section IV the non-commutability of the limiting cases. In Section V, a new basis functions are presented to calculate Mie scattering in the Chandrasekhar-Sekera representation and its implementation for numerical calculation is discussed. Concluding remarks are presented in Section VI.

II. MIE SCATTERING

Let us consider a non-absorbing medium with (real) refractive index n_m ($n_m \in \mathbb{R}$), a sphere of radius a and (complex) refractive index n_s ($n_s \in \mathcal{C}$) to take emission or absorption into account. Here we use the same scattering approach as van de Hulst [1] and Kerker [2], so that $\text{Im}(n_s) \leq 0$. The origin of the laboratory frame ($\hat{x}, \hat{y}, \hat{z}$) is placed at the center of a spherical particle. An incident monochromatic (plane) wave, with electric field \vec{E}_0 and wavelength λ (consequently the wavenumber $k = 2\pi/\lambda$), propagates along the z -direction with wavevector $\vec{k}_0 = k\hat{z}$ and it is scattered by the sphere. The interest is on the spherical scattered field \vec{E}_1 along the \vec{k} direction, defined by the spherical angles θ and ϕ according to the laboratory frame. The scattering plane is formed by the vectors \vec{k}_0 and \vec{k} . Notice that the scattering plane cannot be univocally defined for backward/forward scattering cases. Although the magnetic field (of the electromagnetic wave) does not explicitly appear in the calculation, it has not been neglected since it can always be obtained from the electric fields (due to the consideration of transverse wave).

A. Scattering Plane Representation

In a distance R from the center of the sphere, with $(ka)^2/kR \ll 1$ (far-field approximation), the scattered field is nearly transverse. The electric field lies on the plane orthogonal to \hat{k} formed by the orthogonal directions $\hat{\theta}$ and $\hat{\phi}$, which form the spherical basis. Using $\iota = \sqrt{-1}$ for the imaginary part, the scattered field in the spherical basis is written as:

$$\begin{bmatrix} E_\theta \\ E_\phi \end{bmatrix}_1 = -\iota \frac{e^{-\iota kR}}{kR} J(\mu, \phi) \begin{bmatrix} E_x \\ E_y \end{bmatrix}_0, \quad (1)$$

with $\mu = \cos\theta$, where θ is the scattering angle and ϕ is the azimuthal angle. The Jones matrix is the product of a diagonal matrix (because of the scatterer spherical symmetry), known as scattering matrix with a rotation matrix:

$$J(\mu, \phi) = \begin{bmatrix} S_{\parallel}(\mu) & 0 \\ 0 & S_{\perp}(\mu) \end{bmatrix} \begin{bmatrix} \cos\phi & \sin\phi \\ -\sin\phi & \cos\phi \end{bmatrix}. \quad (2)$$

The rotation matrix projects the incident electric field (given in the laboratory frame) to the parallel and perpendicular directions relative to the scattering plane. The scattering matrix then alters the field values via $S_{\parallel}(\mu)$ and $S_{\perp}(\mu)$, which are the parallel and perpendicular scattering amplitudes (relative to the scattering plane), respectively,

$$S_{\parallel}(\mu) = \sum_{n=1}^{\infty} \frac{2n+1}{n(n+1)} [a_n \tau_n(\mu) + b_n \pi_n(\mu)], \quad (3)$$

$$S_{\perp}(\mu) = \sum_{n=1}^{\infty} \frac{2n+1}{n(n+1)} [a_n \pi_n(\mu) + b_n \tau_n(\mu)], \quad (4)$$

where a_n and b_n are the Mie coefficients [1, 2, 12], and

$$\pi_n(\mu) = \frac{P_n^{(1)}(\mu)}{\sqrt{1-\mu^2}}, \quad (5)$$

$$\tau_n(\mu) = \frac{dP_n^{(1)}(\mu)}{d\theta} = \mu\pi_n(\mu) - (1-\mu^2)\pi_n'(\mu), \quad (6)$$

with $\pi_n'(\mu) = d\pi_n(\mu)/d\mu$ and $P_n^{(1)}(\mu)$ being the n^{th} Legendre polynomial of first order. In practice the summations in n in Eqs. (3) and (4) must be performed to $n_{\text{max}} = ka + 4(ka)^{1/3} + 2$ [46, 47].

The Mie scattering is dependent only on three quantities: the size parameter ka , (complex) relative refractive index $m = n_s/n_m$ ($m \in \mathcal{C}$) and $\tilde{m} = m/\tilde{\mu}$ (relative impedance), where $\tilde{\mu} = \mu_s/\mu_m$ is the relative (sphere/medium) complex magnetic permeability [12–17, 20]. Notice that sphere and medium refractive indices are $n_s = \sqrt{\epsilon_s \mu_s / (\epsilon_0 \mu_0)}$ and $n_m = \sqrt{\epsilon_m \mu_m / (\epsilon_0 \mu_0)}$, where ϵ_0 and μ_0 are the vacuum permittivity and permeability, respectively. The numerical calculation of this scattering event consists of two parts: the first one involving wavelength, relative refractive indices and size of the scatterer (Mie coefficients a_n and b_n , which directly leads to several cross-sections) and the second one involving the scattering angular dependence (scattering amplitudes S_{\parallel} and S_{\perp} , which leads to the phase function).

The calculation of Mie coefficients a_n and b_n depends on ka , m and \tilde{m} through the calculation of spherical Bessel, Neumann, and Hankel functions and their first derivatives with respect to their argument (either ka or mka). The difficulty in this calculation is that the recurrence relationships for complex arguments of the Bessel functions are not stable. This problem is solved writing the spherical functions in the ratio form [48] for Mie coefficients and with the use of the continued fraction method developed by Lentz [49].

If a desired precision in the results is known in advance, it is possible to use the recurrences for a_n and b_n developed by Bohren [50] and implement the scheme proposed by Cachorro [51]. Further improvements to this calculation have been compiled and studied in detail in Ref. [52].

The second part of the calculation concerns the scattered field. It depends on the relative position of the detector with respect to the scatterer and source and also on the distance between scatterer and detector. The scattering amplitudes, which depend on the azimuthal angles, cosine of the scattering angle μ and on the Mie coefficients, can be efficiently calculated using the algorithm created by Wiscombe [47].

Observe that the total scattering cross section is obtained by means of the optical theorem, which is obtained expanding the scattering amplitudes up to second order on the scattering angle.

B. Scattering Amplitudes

The expansions of the scattering amplitudes are presented up to the fourth-order on the scattering angle. These expansions have been explicitly included since they are not easily found in the current literature. As shown in Ref. [2, p. 73], the Legendre polynomials can be written as: $P_n(\cos\theta) = \sum_{p=\delta, \delta+2}^n \mu_n^p \cos^p \theta$, where $\delta = 0(1)$ if n is even (odd) and $\mu_n^p = (-1)^{(n-p)/2} 1 \cdot 3 \cdot 5 \cdots (n+p-1) / \{2^{(n-p)/2} [(n-p)/2]! p!\}$ so that: $P_n^{(1)}(\cos\theta) = \sin\theta dP_n(\cos\theta)/d\cos\theta$ and Eqs. (5) and (6) are rewritten as: $\pi_n(\cos\theta) = \sum_{p=\delta, \delta+2}^n \mu_n^p p \cos^{p-1} \theta$, $\tau_n(\cos\theta) = \cos\theta \pi_n(\cos\theta) - \sin^2 \theta \pi_n'(\cos\theta) = \sum_{p=\delta, \delta+2}^n \mu_n^p p \cos^{p-2} \theta (1 - p \sin^2 \theta)$.

1. Expansion along the Forward/Backward Direction

Using the following sum rules:

$$H_n^{(\pm)} = \sum_{p=\delta, \delta+2}^n (\pm 1)^{p-1} \mu_n^p p = \frac{(\pm 1)^{n+1} n(n+1)}{2}, \quad (7)$$

$$K_n^{(\pm)} = \sum_{p=\delta, \delta+2}^n (\pm 1)^{p-1} \mu_n^p p^2 = \frac{H_n^{(\pm)}}{2} [1 + (\pm 1)^{n+1} H_n^{(\pm)}] \\ = \frac{[n(n+1) + 2]}{4} H_n^{(\pm)}, \quad (8)$$

and expanding the $\pi_n(\mu)$ and $\tau_n(\mu)$ functions up to $O(\theta^4)$ around the back and forward scattering directions

$$\frac{\pi_n(\mu \rightarrow \pm 1)}{H_n^{(\pm)}} = 1 + \left[1 - \frac{n(n+1)}{2} \right] \frac{\theta^2}{4} + \dots, \quad (9)$$

$$\frac{\tau_n(\mu \rightarrow \pm 1)}{\pm H_n^{(\pm)}} = 1 + \left[1 - \frac{3n(n+1)}{2} \right] \frac{\theta^2}{4} + \dots \quad (10)$$

one obtains the forwards/backwards scattering amplitudes:

$$S_{\parallel}(\mu \rightarrow \pm 1) = S(\pm 1) + L^{(\pm)} \theta^2 + \dots, \quad (11)$$

$$S_{\perp}(\mu \rightarrow \pm 1) = \pm S(\pm 1) + P^{(\pm)} \theta^2 + \dots, \quad (12)$$

where

$$S(\pm 1) = \sum_{n=1}^{\infty} S_n^{(\pm)}(b_n \pm a_n), \quad (13)$$

$$8L^{(\pm)} = \sum_{n=1}^{\infty} S_n^{(\pm)} [2(b_n \pm a_n) - n(n+1)(b_n \pm 3a_n)]/4$$

$$8P^{(\pm)} = \sum_{n=1}^{\infty} S_n^{(\pm)} [2(a_n \pm b_n) - n(n+1)(a_n \pm 3b_n)]/5$$

$$S_n^{(\pm)} = \frac{2n+1}{n(n+1)} H_n^{(\pm)}. \quad (16)$$

From Eqs. (11) and (12), one obtains the following properties for the exact forward amplitude, which is used to calculate the total scattering cross section using the optical theorem: $S_{\perp}(1) = S_{\parallel}(1)$ and backward scattering amplitude, which gives the backscattering (radar) cross section [1–4], $S_{\perp}(-1) = -S_{\parallel}(-1)$. For future use, let us define the following quantity

$$\Delta^{(\pm)} = \pm P^{(\pm)} - L^{(\pm)} \\ = \frac{1}{4} \sum_{n=1}^{\infty} (2n+1) H_n^{(\pm)} (\pm a_n - b_n), \quad (17)$$

where $H_n^{(\pm)}$ is given by Eq. (7).

2. Expansion for Small Particle Size

The general Mie coefficients for the magnetic case has been pointed out in Ref. [12] and in the limit of small-particle, the size parameter $ka \ll 1$, they are [13]:

$$a_1 = \frac{\gamma}{2} \frac{ka - 2\tilde{m}A_1(mka)}{ka + \tilde{m}A_1(mka)} \quad (18)$$

$$b_1 = \frac{\gamma}{2} \frac{\tilde{m}ka - 2A_1(mka)}{\tilde{m}ka + A_1(mka)}, \quad (19)$$

where $\gamma = -2i(ka)^3/3$, $A_1(z) = \psi_1(z)/\psi_1'(z)$ and $\psi_1(z) = zj_1(z)$ is the spherical Bessel-Riccati function ($j_1(z) = \sin z/z^2 - \cos z/z$) and prime means the derivative with respect to the argument of the function. This is the general magnetic scattering by small particles.

To ensure the Rayleigh scattering, the wavelength must also be small inside the scatterer $|m|ka \ll 1$ leading to [12]

$$a_1 = \gamma \frac{1 - \tilde{\epsilon}}{2 + \tilde{\epsilon}} \quad (20)$$

$$b_1 = \gamma \frac{1 - \tilde{\mu}}{2 + \tilde{\mu}}, \quad (21)$$

where $\tilde{\epsilon}$ and $\tilde{\mu}$ are relative (sphere to medium) permittivity and permeability. Notice that the whole magnetic dependence is in the b_1 term, which vanishes for non-magnetic scattering ($\tilde{\mu} = 1$).

Next the auxiliary quantities are written in the small-particle limit

$$S(\pm 1) = \frac{3}{2}(b_1 \pm a_1), \quad (22)$$

$$L(\pm) = \frac{\mp 3}{4} a_1, \quad (23)$$

$$P(\pm) = \frac{\mp 3}{4} b_1, \quad (24)$$

$$\Delta(\pm) = \frac{3}{4}(\pm a_1 - b_1), \quad (25)$$

where near forward/backward scattering, the parallel scattering amplitude is influenced only by an electric component $L(\pm)$ and the perpendicular one only by the magnetic correction $P(\pm)$.

III. CHANDRASEKHAR-SEKERA REPRESENTATION

With the scattering plane representation one can express directly the photon “history” from the source to the detector. Nevertheless, for multiple scattering it presents some inconveniences. From one scattering event to another, the electric field needs to be written in local basis. The $\kappa + 1$ scattering event is written in the preceding $(\hat{\theta}_\kappa, \hat{\phi}_\kappa, \hat{k}_\kappa)$ basis, which depends on the photon history as illustrated by Fig. 1. For instance, to write the scattered field along a scattering sequence in a Monte Carlo scheme, the azimuthal and scattering angles and all the distances along the sequence need to be recorded to perform the right basis transformation back to the laboratory (fixed) frame. This bookkeeping is necessary when the reversed scattering sequences must be obtained. This representation becomes specially cumbersome for the calculation of the coherent backscattering enhancement (weak localization of light) [13–16, 45].

The difficulties presented above can be solved using the Chandrasekhar-Sekera representation [42, 43]. Consider for example the κ^{th} scattering event in a given scattering sequence. As previously, an incident monochromatic (plane) wave with wavevector \vec{k}_κ is considered and one is interested in the scattered field along the direction $\vec{k}_{\kappa+1}$. Note that in this case the incident direction is arbitrary, not necessarily along the \hat{z} -direction, as in the scattering plane representation. In a distance $R_{\kappa+1}$ from the center of the sphere, with $(ka)^2/kR_{\kappa+1} \ll 1$ (far-field approximation), the scattered field is nearly transverse and the electric field lies on the plane formed by the spherical basis vectors $\hat{\Theta}_{\kappa+1}$ and $\hat{\Phi}_{\kappa+1}$. The spherical basis $(\hat{\Theta}_\kappa, \hat{\Phi}_\kappa, \hat{k}_\kappa)$ is defined by the angle Θ_κ , which is obtained from the projection of the wavevector \vec{k}_κ along the \hat{z} -direction ($\cos \Theta_\kappa = \hat{k}_\kappa \cdot \hat{z}$) and by the azimuthal

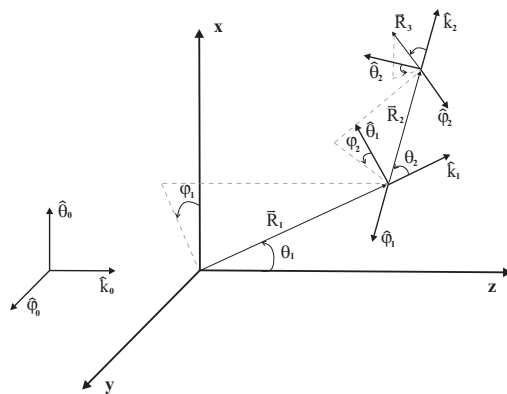


FIG. 1: Sequence of three scattering events where the Chandrasekhar-Sekera basis are explicitly shown.

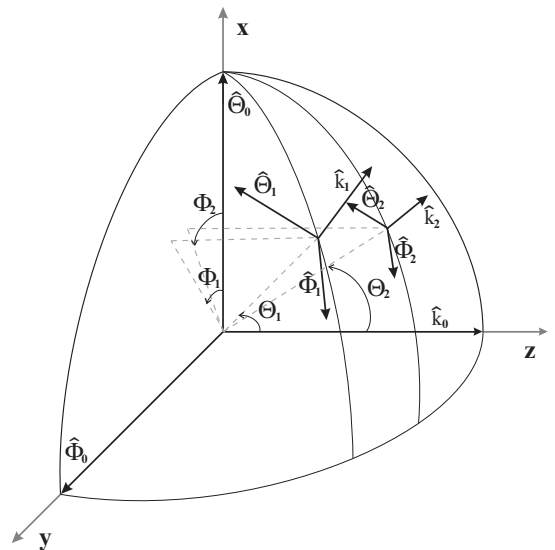


FIG. 2: Angles in the Chandrasekhar-Sekera representation along the scattering sequence of Fig. 1.

angle Φ_κ , which is counted from \hat{x} to the projection of \vec{k}_κ onto xy -plane, relative to the laboratory frame, as shown in Fig. 2.

Equivalently to the scattering plane representation, one can write the scattered electric field $\vec{E}_{\kappa+1}$ along the directions $(\hat{\Theta}_{\kappa+1}, \hat{\Phi}_{\kappa+1})$ as a function of the incident field \vec{E}_κ along the directions $(\hat{\Theta}_\kappa, \hat{\Phi}_\kappa)$:

$$\vec{E}_{\kappa+1}(\hat{k}_{\kappa+1}) = -i \frac{e^{-i k R_{\kappa+1}}}{k R_{\kappa+1}} J(\hat{k}_{\kappa+1}, \hat{k}_\kappa) \vec{E}_\kappa(\hat{k}_\kappa), \quad (26)$$

where the Jones matrix is:

$$J(\hat{k}_{\kappa+1}, \hat{k}_{\kappa}) = \begin{bmatrix} (l, l) & (l, r) \\ -(l, r) & (l, l) \end{bmatrix} \begin{bmatrix} X_1 & 0 \\ 0 & X_2 \end{bmatrix} + \begin{bmatrix} -(r, l) & (r, r) \\ (r, r) & (r, l) \end{bmatrix} \begin{bmatrix} 0 & X_1 \\ X_2 & 0 \end{bmatrix}, \quad (27)$$

$$(l, l) = \sqrt{(1 - \mu_{\kappa}^2)(1 - \mu_{\kappa+1}^2)} + \mu_{\kappa}\mu_{\kappa+1} \cos(\Delta\Phi_{\kappa, \kappa+1}), \quad (28)$$

$$(l, r) = -\mu_{\kappa} \sin(\Delta\Phi_{\kappa, \kappa+1}), \quad (29)$$

$$(r, l) = \mu_{\kappa+1} \sin(\Delta\Phi_{\kappa, \kappa+1}), \quad (30)$$

$$(r, r) = \cos(\Delta\Phi_{\kappa, \kappa+1}), \quad (31)$$

$$\Delta\Phi_{\kappa, \kappa+1} = \Phi_{\kappa} - \Phi_{\kappa+1}, \quad (32)$$

$$\mu_{\kappa} = \cos \Theta_{\kappa}, \quad (33)$$

where the azimuthal scattering angle is $\Delta\Phi_{\kappa, \kappa+1}$ (equivalent to ϕ in the scattering plane representation). The notation of Eq. (218) in Ref. [42, p. 38-43] has been kept in this calculation and the geometrical interpretation obtained from the spherical triangle shown in Fig. 8 of Ref. [42, p. 39]. The modified scattering amplitudes, which depend only on the cosine of the scattering angle μ due to the spherical symmetry of the scatterer, are defined by

$$X_1(\mu) = \frac{S_{\perp}(\mu) - \mu S_{\parallel}(\mu)}{1 - \mu^2}, \quad (34)$$

$$X_2(\mu) = \frac{S_{\parallel}(\mu) - \mu S_{\perp}(\mu)}{1 - \mu^2}, \quad (35)$$

$$\begin{aligned} \mu &= \cos \theta = (l, l)(r, r) - (l, r)(r, l) \\ &= \sqrt{(1 - \mu_{\kappa}^2)(1 - \mu_{\kappa+1}^2)} \cos(\Delta\Phi_{\kappa, \kappa+1}) + \mu_{\kappa}\mu_{\kappa+1} \end{aligned} \quad (36)$$

with the scattering amplitudes given by Eqs. (3) and (4). Because of the basis transformations, the Jones matrix in the Chandrasekhar-Sekera representation Eq. (27) cannot simply be written as product of a scattering by a rotation matrix as in the scattering plane representation [Eq. (2)]. Nevertheless, writing $\hat{k}_{\kappa} = \hat{z}$, $\hat{\Theta}_{\kappa} = \hat{x}$, and $\hat{\Phi}_{\kappa} = \hat{y}$, then $\Phi_{\kappa} = 0$, and $\Theta_{\kappa} = 0$ for the incident direction and $\Phi_{\kappa+1} = \phi$, and $\Theta_{\kappa+1} = \theta$, then $\Delta\Phi_{\kappa, \kappa+1} = -\phi$, $\mu_{\kappa} = 1$, and $\mu_{\kappa+1} = \cos \theta$, the scattering plane representation can be obtained as a particular case.

Although the Chandrasekhar-Sekera representation is more complex than the scattering plane representation, it is suitable for numerical calculation in the multiple scattering context since it already includes the basis transformation in itself. In this representation, given \hat{k}_{κ} and $\hat{k}_{\kappa+1}$ in the laboratory frame, the electric field along the scattering sequence can be promptly obtained, even in the case where the reverse sequences must be calculated such as in the weak localization of electromagnetic waves.

IV. NON-COMMUTABILITY OF LIMITING CASES

To calculate the scattering of light by polydispersions, particle size may range from the small particle to large sphere limit. Numerical problems with Eqs. (34) and (35) may occur since forward/backward scattering events ($\mu \rightarrow \pm 1$) have non-vanishing probability.

Backward/forward scattering are important in practice. For instance, the phase functions are very forwardly peaked ($\mu \rightarrow 1$) in the Mie regime. In lidar calculation, the interest is in the backward scattering events ($\mu \rightarrow -1$, in general these scattering events are forced to occur by Metropolis variance-reduction methods in a Monte Carlo scheme).

Since these difficulties have never been reported in the literature, they are explicitly developed here, where we consider the particles to be magnetic. The non-magnetic approach, which is widely applied in the optical frequency ranges for all materials, can be readily obtained by assuming $\tilde{\mu} = \mu_s/\mu_m = 1$ in our expressions.

A simple way to obtain the limiting values, which works properly for the optical theorem, is to rewrite Eqs. (34) and (35) as: $X_1(\mu) = [S_{\perp}(\mu) - \mu S_{\parallel}(\mu)]/[(1 + \mu)(1 - \mu)]$ and $X_2(\mu) = [S_{\parallel}(\mu) - \mu S_{\perp}(\mu)]/[(1 + \mu)(1 - \mu)]$.

In the forward/backward limiting cases of $\mu \rightarrow \pm 1$, $S_{\perp}(1) = S_{\parallel}(1) = S(1)$, $S_{\perp}(-1) = -S(-1)$ and $S_{\parallel}(-1) = S(-1)$, with $S(\pm 1)$ given by Eq. (13), and one can write: $X_1(\mu \rightarrow \pm 1) = \pm S(\pm 1)/2$ and $X_2(\mu \rightarrow \pm 1) = S(\pm 1)/2$. In short, $X_1(\pm 1) = \pm X_2(\pm 1)$.

Now let us consider the limit $ka \rightarrow 0$ (small-particle limit), and the leading Mie coefficients are $a_1 = 2i\alpha(ka)^3/3$ and $b_1 = 2i\beta(ka)^3/3$, with $\alpha = (\tilde{\epsilon} - 1)/(\tilde{\epsilon} + 2)$ and $\beta = (\tilde{\mu} - 1)/(\tilde{\mu} + 2)$ [12]. From Eqs. (3) and (4), the scattering amplitudes are $S_{\perp}(\mu) = i(\alpha + \mu\beta)(ka)^3$ (independent of μ when $\tilde{\mu} = 1$) and $S_{\parallel}(\mu) = i(\mu\alpha + \beta)(ka)^3$, and so that: $X_1(\mu) = i\alpha(ka)^3$ and $X_2(\mu) = i\beta(ka)^3$. For $\beta = 0$ and $\mu \rightarrow 1$, this implies $X_1(1) = S_{\perp} = S_{\parallel}$ and $X_2(1) = 0$, leading to $X_1(\pm 1) \neq \pm X_2(\pm 1)$.

Formally, in the non-magnetic approach ($\beta = 0$), X_1 tends to zero, as ka tends to zero, while X_2 vanishes. Taking the limit $\mu \rightarrow \pm 1$ and then $ka \rightarrow 0$ the result is different than taking $ka \rightarrow 0$ and then $\mu \rightarrow \pm 1$. These limits do not commute, which is a non-physical result. Furthermore, the order the limits are taken affects numerical results.

Once this problem has been noticed, the solution is obvious: expand the scattering amplitudes to higher-order terms as function of $\mu = \cos \theta$. Because of the presence of a $1 - \mu^2 = \sin^2 \theta$ in the denominator of $X_1(\mu)$ and $X_2(\mu)$ [Eqs. (34) and (35)], the consideration up to fourth-order terms in θ is mandatory here, in contrast to the use of the optical theorem.

For $\mu \rightarrow \pm 1$, using Eqs. (11), (12), (34) and (35), one

obtains:

$$X_1(\mu \rightarrow \pm 1) = \pm \frac{S(\pm 1)}{2} \pm \Delta^{(\pm)},$$

$$X_2(\mu \rightarrow \pm 1) = \frac{S(\pm 1)}{2} - \Delta^{(\pm)},$$

where $\Delta^{(\pm)}$ is given by Eq. (17) and which corrects the problem of non-commutability of limits. For small particle scattering, $\Delta^{(\pm)} = \imath(\mp\alpha - \beta)(ka)^3/2$, which leads to the correct values: $X_1 = \imath\alpha(ka)^3$ and $X_2 = \imath\beta(ka)^3$.

V. THE NEW SET OF BASIS FUNCTIONS

An effective manner to solve the non-commutability of the limiting cases is to use the definitions of the scattering amplitudes [Eqs. (3) and (4)] and rewrite $X_1(\mu)$ and $X_2(\mu)$ in Eqs. (34) and (35) as:

$$X_1(\mu) = \sum_{n=1}^{\infty} \frac{2n+1}{n(n+1)} [a_n \chi_n^{(1)}(\mu) + b_n \chi_n^{(2)}(\mu)] \quad (37)$$

$$X_2(\mu) = \sum_{n=1}^{\infty} \frac{2n+1}{n(n+1)} [a_n \chi_n^{(2)}(\mu) + b_n \chi_n^{(1)}(\mu)] \quad (38)$$

$$\chi_n^{(1)}(\mu) = \frac{\pi_n(\mu) - \mu\tau_n(\mu)}{1 - \mu^2} = \pi_n(\mu) + \mu\pi'_n(\mu) \quad (39)$$

$$\chi_n^{(2)}(\mu) = \frac{\tau_n(\mu) - \mu\pi_n(\mu)}{1 - \mu^2} = -\pi'_n(\mu), \quad (40)$$

where Eqs. (5) and (6) have been used.

Instead of calculating the scattering amplitudes $S_{\perp}(\mu)$ and $S_{\parallel}(\mu)$, $X_1(\mu)$ and $X_2(\mu)$ can be directly calculated from the basis functions $\chi_n^{(1)}(\mu)$ and $\chi_n^{(2)}(\mu)$. The consideration of Eqs. (39) and (40) implies to an important achievement, since the term $\sin^2\theta$ that appears in the denominator of Eqs. (34) and (35) cancels out when one writes $\tau_n(\mu) = \mu\pi_n(\mu) - (1 - \mu^2)\pi'_n(\mu)$ [Eq. (6)]. In this way, no asymptotic behavior for $X_1(\mu)$ and $X_2(\mu)$ must be explicitly calculated numerically, avoiding numerical tests, which increase computer time. This procedure achieves directly the limiting cases, independently of the order these limits are taken.

The functions $\pi_n(\mu)$ and $\pi'_n(\mu)$ can be obtained numerically by stable recursion relations [2, 47]

$$t_{n-1}(\mu) = (2n-1)\pi_{n-1}(\mu) \quad (41)$$

$$\pi'_n(\mu) = t_{n-1}(\mu) + \pi'_{n-2}(\mu) \quad (42)$$

$$\pi_n(\mu) = \frac{\mu t_{n-1}(\mu) - n\pi_{n-2}(\mu)}{n-1}, \quad (43)$$

which are initialized with $\pi_0(\mu) = 0$, $\pi_1(\mu) = 1$, $\pi_2(\mu) = 3\mu$, $\pi'_1(\mu) = 0$ and $\pi'_2(\mu) = 3$.

A further improvement can be achieved in numerical calculations. Instead of using $X_1(\mu)$ and $X_2(\mu)$, one

writes:

$$X_{\pm}(\mu) = \frac{X_1(\mu) \pm X_2(\mu)}{2}$$

$$= \frac{1}{2} \sum_{n=1}^{\infty} \frac{2n+1}{n(n+1)} (a_n \pm b_n) \chi_n^{(\pm)}(\mu) \quad (44)$$

$$\chi_n^{(\pm)}(\mu) = \chi_n^{(1)}(\mu) \pm \chi_n^{(2)}(\mu), \quad (45)$$

which is an adaptation of the Wiscombe's method [47]. For small particle scattering $X_{\pm}(\mu) = \imath(\alpha \pm \beta)(ka)^3/2$, which leads to the correct limits $X_1 = \imath\alpha(ka)^3$ and $X_2 = \imath\beta(ka)^3$.

In brief the new algorithm works as follows. Given the size parameter ka , the relative refraction index m and \tilde{m} (for magnetic scattering), one calculates the Mie coefficients a_n and b_n and store the terms $(2n+1)(a_n \pm b_n)/[2n(n+1)]$ [Eq. (44)] in arrays [47]. Given the input \hat{k}_{κ} and output $\hat{k}_{\kappa+1}$ directions, proceed as follows:

1. obtain the scattering angle as given by Eq. (36);
2. calculate the ‘‘Legendre’’ polynomials by the recursion relationships of Eqs. (41,) (42) and (43,);
3. the basis functions $\chi_n^{\pm}(\mu)$ are obtained by Eq. (45);
4. $X_{\pm}(\mu)$, $X_1(\mu)$ and $X_2(\mu)$ are given by Eqs. (44), (37) and (38);
5. the azimuthal angle is calculated with Eq. (32);
6. the director cosines are obtained by Eq. (33);
7. use Eqs. (28), (29), (30) and (31) to obtain (l, l) , (l, r) , (r, l) and (r, r) , respectively;
8. the results of the above items permit the calculations of the Jones matrix with Eq. (27),
9. and finally, at the distance $R_{\kappa+1}$ from the center of the sphere along $\hat{k}_{\kappa+1}$, the scattered electric field is given by Eq. (26).

The calculations are performed on the field level. To obtain the Stokes intensities (I , Q , U and V) use the coherence matrix $\vec{E}_{\kappa+1}^{\dagger} \vec{E}_{\kappa+1}$ [45].

For a fixed particle size (monodispersions), the functions $\chi_n^{(\pm)}(\mu)$ are calculated each time the angles of source and detection are modified, or when a new scattering event occurs in a Monte Carlo sequence. In this case, it is suitable to tabulate $X_{\pm}(\mu)$ [Eq. (44)], in uneven partitions. Higher resolution are required for $|\mu|$ close to unity [46], roughly $\theta < ka$ in the forward case and $\pi - \theta < (ka)^{4/3}$ in the backward case. To consider polydispersions, the size-distribution function must be taken into account. Some of these size-distribution functions are found in Ref. [53] and an implementation for large size parameters is found in Ref. [54]. In this case, values of $\langle |X_{+}(\mu)|^2 \rangle$, $\langle |X_{-}(\mu)|^2 \rangle$, $\text{Re}[\langle X_{+}(\mu) X_{-}^*(\mu) \rangle]$ and $\text{Im}[\langle X_{+}(\mu) X_{-}^*(\mu) \rangle]$ should be tabulated, where $\langle \dots \rangle$ refers to the size-distribution average.

VI. CONCLUSION

The Chandrasekhar-Sekera representation is more appropriate than the scattering plane representation to be considered when multiple Mie scattering of light is taken into account. Nevertheless, care must be taken when this representation is used because of the non-commutability of the limiting cases of Rayleigh and forward/backward scattering. It must be corrected considering the higher-order terms in the scattering angle in the scattering amplitude expansions. A new set of basis functions for the calculation of the angular functions in the Mie scattering in the Chandrasekhar-Sekera representation has been presented. An effective algorithm has been implemented using new basis functions, which have been introduced.

Furthermore, the use of a generalization (to associated Legendre polynomials) of $\chi_n^{(1)}$ and $\chi_n^{(2)}$ can be used for

non-spherical scattering, such as in the extended boundary condition presented in Ref. [55]. This generalization, among the generalization for the spherical Henkel functions, allows the writing of the scattering amplitudes of non-spherical particles in terms of matrices, which are suitable for numerical calculations. These calculations will be reported in future.

Acknowledgement

ASM acknowledges the support from the Brazilian agency CNPq (303990/2007-4). TJA acknowledges the support from the Brazilian agency FAPESP (2010/10052-0). The authors thank the very stimulating discussions with Felipe Arruda Pinheiro.

-
- [1] H. C. van de Hulst, *Light Scattering by Small Particles*, Dover, New York, 1980.
 - [2] M. Kerker, *The Scattering of Light and Other Electromagnetic Radiation*, Academic Press, New York, 1969.
 - [3] C. F. Bohren, D. R. Huffman, *Absorption and Scattering of Light by Small Particles*, John Wiley, New York, 1983.
 - [4] M. I. Mishchenko, L. D. Travis, A. A. Lacis, *Scattering, Absorption, and Emission of Light by Small Particles*, Cambridge University Press, Cambridge, 2002.
 - [5] G. Videen, Y. Yatskiv, M. I. Mishchenko (Eds.), *Photopolarimetry in Remote Sensing*, Kluwer Academic Publishers, Dordrecht, 2004.
 - [6] E. Wolf, T. Habashy, Invisible bodies and uniqueness of the inverse scattering problem, *Journal of Modern Optics* 40 (1993) 785–792.
 - [7] J. D. Klett, Stable analytical inversion solution for processing lidar returns, *Appl. Opts.* 20 (1981) 211–219.
 - [8] M. T. Chahine, Inverse problems in radiative transfer: determination of atmospheric parameters, *J. Atmos. Sci.* 27 (1970) 960–967.
 - [9] H. Y. Li, C. Y. Yang, A genetic algorithm for inverse radiation problems, *Int. J. Heat Mass Transfer* 40 (1997) 1545–1549.
 - [10] M. M. Sigalas, C. M. Soukoulis, R. Biswas, K. M. Ho, Effect of the magnetic permeability on photonic band gaps, *Phys. Rev. B* 56 (1997) 959–962.
 - [11] W. Zhang, C. T. Chan, P. Sheng, Multiple scattering theory and its application to photonic band gap systems consisting of coated spheres, *Opt. Express* 8 (3) (2001) 203–208.
 - [12] M. Kerker, D. S. Wang, C. L. Giles, Electromagnetic scattering by magnetic spheres, *J. Opt. Soc. Am.* 73 (6) (1983) 765–767.
 - [13] F. A. Pinheiro, A. S. Martinez, L. C. Sampaio, New effects in light scattering in disordered media and coherent backscattering cone: Systems of magnetic particles, *Phys. Rev. Lett.* 84 (7) (2000) 1435–1438.
 - [14] F. A. Pinheiro, A. S. Martinez, L. C. Sampaio, Vanishing of energy transport velocity and diffusion constant of electromagnetic waves in disordered magnetic media, *Phys. Rev. Lett.* 85 (26) (2000) 5563–5566.
 - [15] F. A. Pinheiro, A. S. Martinez, L. C. Sampaio, Electromagnetic scattering by small particles, *J. Magn. Magn. Mater.* 1951 (2001) 226–230.
 - [16] F. A. Pinheiro, A. S. Martinez, L. C. Sampaio, Multiple scattering of magnetic waves in disordered magnetic media: Localization parameter, energy transport velocity and diffusion constant, *Braz. J. Phys.* 31 (1) (2001) 65–70.
 - [17] R. V. Mehta, R. Patel, R. Desai, R. V. Upadhyay, K. Parekh, Experimental evidence of zero forward scattering by magnetic spheres, *Physical Review Letters* 96 (12) (2006) 127402.
 - [18] Y. L. Kim, P. Pradhan, M. H. Kim, V. Backman, Circular polarization memory effect in low-coherence enhanced backscattering of light, *Opt. Lett.* 31 (18) (2006) 2744–2746.
 - [19] R. V. Mehta, R. Patel, R. V. Upadhyay, Direct observation of magnetically induced attenuation and enhancement of coherent backscattering of light, *Phys. Rev. B* 74 (19) (2006) Art. No. 195127.
 - [20] T. J. Arruda, A. S. Martinez, Electromagnetic energy within magnetic spheres, *J. Opt. Soc. Am. A* 27 (2010) 992–1001.
 - [21] T. J. Arruda, A. S. Martinez, Electromagnetic energy within a magnetic infinite cylinder and scattering properties for oblique incidence, *J. Opt. Soc. Am. A* 27 (2010) 1679–1687.
 - [22] P. Sheng (Ed.), *Scattering and Localization of Classical Wave Localization in Random Media*, World Scientific Publishing, Singapore, 1990.
 - [23] F. C. MacKintosh, J. X. Zhu, D. J. Pine, D. A. Weitz, Polarization memory of multiply scattered-light, *Phys. Rev. B* 40 (13) (1989) 9342–9345.
 - [24] D. Bicout, C. Brosseau, A. S. Martinez, J. M. Schmitt, Depolarization of multiply scattered waves by spherical diffusers: Influence of the size parameter, *Phys. Rev. E* 49 (2) (1994) 1767–1770.
 - [25] M. Xu, R. R. Alfano, Random walk of polarized light in turbid media, *Phys. Rev. Lett.* 95 (21) (2005) 213901.

- [26] M. Xu, R. R. Alfano, Circular polarization memory of light, *Phys. Rev. E* 72 (6) (2005) 065601.
- [27] E. E. Gorodnichenov, A. I. Kuzovlev, D. B. Rogozkin, Depolarization of multiply scattered light in transmission through a turbid medium with large particles, *Opt. Comm.* 260 (1) (2006) 30–45.
- [28] A. Legendijk, B. A. van Tiggelen, Resonant multiple scattering of light, *Phys. Rep.* 270 (3) (1996) 143–215.
- [29] P. R. Group (Ed.), *New Aspects of Electromagnetic and Acoustic Wave Diffusion*, Vol. 144 of Springer Tracts in Modern Physics, Springer-Verlag, Berlin, 1998.
- [30] M. I. Mishchenko, L. D. Travis, A. A. Lacis, *Multiple Scattering of Light by Particles: Radiative Transfer and Coherent Backscattering*, Cambridge University Press, Cambridge, 2006.
- [31] N. Ghosh, S. K. Majumder, P. K. Gupta, Polarized fluorescence spectroscopy of human tissues, *Opt. Lett.* 27 (22) (2002) 2007–2009.
- [32] D. A. Zimnyakov, V. V. Tuchin, Optical tomography of tissues, *Quantum Electronics* 32 (10) (2002) 849–867.
- [33] V. Sankaran, J. T. Walsh, D. J. Maitland, Comparative study of polarized light propagation in biologic tissues, *J. Biomed. Opt.* 7 (3) (2002) 300–306.
- [34] C. W. Sun, C. C. Yang, Y. W. Kiang, Optical imaging based on time-resolved Stokes vectors in filamentous tissues, *Appl. Optics* 42 (4) (2003) 750–754.
- [35] N. Ghosh, P. K. Gupta, H. S. Patel, B. Jain, B. N. Singh, Depolarization of light in tissue phantoms - effect of collection geometry, *Opt. Commun.* 222 (1-6) (2003) 93–100.
- [36] N. Ghosh, H. S. Patel, P. K. Gupta, Depolarization of light in tissue phantoms - effect of a distribution in the size of scatterers, *Opt. Express* 11 (18) (2003) 2198–2205.
- [37] J. H. Ali, W. B. Wang, M. Zevallos, R. R. Alfano, Near infrared spectroscopy and imaging to probe differences in water content in normal and cancer human prostate tissues, *Technology in Cancer Research & Treatment* 3 (5) (2004) 491–497.
- [38] Y. Liu, Y. L. Kim, X. Li, V. Backman, Investigation of depth selectivity of polarization gating for tissue characterization, *Opt. Express* 13 (2) (2005) 601–611.
- [39] O. V. Angelsky, A. G. Ushenko, D. N. Burkovets, Y. A. Ushenko, Polarization visualization and selection of biotissue image two-layer scattering medium, *J. Biomed. Opts.* 10 (1) (2005) 014010.
- [40] S. Gupta, M. S. Nair, A. Pradhan, N. C. Riswal, N. Agarwal, A. Agarwal, P. K. Panigrahi, Wavelet-based characterization of spectral fluctuations in normal, benign, and cancerous human breast tissues, *J. Biomed. Opt.* 10 (5) (2005) 054012.
- [41] M. Itoh, M. Yamanari, Y. Yasuno, T. Yatagai, Polarization characteristics of multiple backscattering in human blood cell suspensions, *Optical and Quantum Electronics* 37 (13-15) (2005) 1277–1285.
- [42] S. Chandrasekhar, *Radiative Transfer*, Dover Publications, New York, 1960.
- [43] Z. Sekera, *J. Opt. Soc. Am* 56 (1966) 1732.
- [44] R. L. T. Cheung, A. Ishimaru, Transmission, backscattering, and depolarization of waves in randomly distributed spherical particles, *App. Opt.* 21 (1982) 3792–3798.
- [45] A. S. Martinez, R. Maynard, Faraday effect and multiple scattering of light, *Phys. Rev. B* 50 (6) (1994) 3714–3732.
- [46] H. M. Nussenzveig, *Diffraction Effects in Semiclassical Scattering*, Cambridge University Press, Cambridge, 1992.
- [47] W. J. Wiscombe, Improved Mie scattering algorithms, *Appl. Opt.* 19 (9) (1980) 1505–1509.
- [48] G. Grehan, G. Gousbet, Mie theory: new progress, with emphasis on particle sizing, *App. Opt.* 18 (1979) 3489–3493.
- [49] W. J. Lentz, Generating bessel functions in mie scattering calculations using continued fractions, *App. Opt.* 15 (1976) 668–671.
- [50] C. F. Bohren, Recurrence relations for the mie scattering coefficients, *J. Opt. Soc. Am.* 4 (1987) 612–613.
- [51] V. E. Cachorro, New improvements for mie scattering calculations, *Journal of Electromagnetic Wave and Applications* 5 (1991) 913–926.
- [52] H. Du, Mie-scattering calculation, *Apl. Opt.* 43 (9) (2004) 1951–1956.
- [53] D. Deirmendjian, *Electromagnetic Scattering on Spherical Polydispersions*, American Elsevier Publishing, New York, 1969.
- [54] S. Wolf, N. V. Voshchinnikov, Mie scattering by ensembles of particles with very large size parameters, *Comp. Phys. Comm.* 162 (2004) 113–123.
- [55] P. W. Barber, S. C. Hill, *Light Scattering by Particles: Computational Methods*, World Scientific, Singapore, 1990.